Mod Pathol 37 (2024) 100416

MODERN PATHOLOGY

USCAP UNITED STATES AND CANADIAN ACADEMY OF PATHOLOGY
Creating a Better Pathologist

Journal homepage: https://modernpathology.org/

Research Article

Artificial Intelligence-Based Mitosis Scoring in Breast Cancer: Clinical Application

Asmaa Ibrahim[a,b], Mostafa Jahanifar[c], Noorul Wahab[c], Michael S. Toss[a,d], Shorouk Makhlouf[a], Nehal Atallah[a], Ayat G. Lashen[a], Ayaka Katayama[a], Simon Graham[c], Mohsin Bilal[c], Abhir Bhalerao[c], Shan E. Ahmed Raza[c], David Snead[e], Fayyaz Minhas[c], Nasir Rajpoot[c,*], Emad Rakha[a,f,g,*]

[a] *Academic Unit for Translational Medical Sciences, School of Medicine, University of Nottingham, Nottingham, United Kingdom;* [b] *Department of Pathology, Faculty of Medicine, Suez Canal University, Egypt;* [c] *Tissue Image Analytics Centre, University of Warwick, United Kingdom;* [d] *Histopathology Department, Royal Hallamshire Hospital, Sheffield Teaching Hospitals NHS Foundation Trust, Sheffield, United Kingdom;* [e] *Cellular Pathology, University Hospitals Coventry and Warwickshire NHS Trust, United Kingdom;* [f] *Nottingham University Hospitals NHS Trust, Nottingham, United Kingdom;* [g] *Pathology Department, Hamad Medical Corporation, Doha, Qatar*

ARTICLE INFO

Article history:
Received 16 June 2023
Revised 27 October 2023
Accepted 14 December 2023
Available online 27 December 2023

Keywords:
algorithm
artificial intelligence
mitosis

ABSTRACT

In recent years, artificial intelligence (AI) has demonstrated exceptional performance in mitosis identification and quantification. However, the implementation of AI in clinical practice needs to be evaluated against the existing methods. This study is aimed at assessing the optimal method of using AI-based mitotic figure scoring in breast cancer (BC). We utilized whole slide images from a large cohort of BC with extended follow-up comprising a discovery ($n = 1715$) and a validation ($n = 859$) set (Nottingham cohort). The Cancer Genome Atlas of breast invasive carcinoma (TCGA-BRCA) cohort ($n = 757$) was used as an external test set. Employing automated mitosis detection, the mitotic count was assessed using 3 different methods, the mitotic count per tumor area (MCT; calculated by dividing the number of mitotic figures by the total tumor area), the mitotic index (MI; defined as the average number of mitotic figures per 1000 malignant cells), and the mitotic activity index (MAI; defined as the number of mitotic figures in 3 mm^2 area within the mitotic hotspot). These automated metrics were evaluated and compared based on their correlation with the well-established visual scoring method of the Nottingham grading system and Ki67 score, clinicopathologic parameters, and patient outcomes. AI-based mitotic scores derived from the 3 methods (MCT, MI, and MAI) were significantly correlated with the clinicopathologic characteristics and patient survival ($P < .001$). However, the mitotic counts and the derived cutoffs varied significantly between the 3 methods. Only MAI and MCT were positively correlated with the gold standard visual scoring method used in Nottingham grading system ($r = 0.8$ and $r = 0.7$, respectively) and Ki67 scores ($r = 0.69$ and $r = 0.55$, respectively), and MAI was the only independent predictor of survival ($P < .05$) in multivariate Cox regression analysis. For clinical applications, the optimum method of scoring mitosis using AI needs to be considered. MAI can provide reliable and reproducible results and can accurately quantify mitotic figures in BC.

These authors contributed equally: Asmaa Ibrahim and Mostafa Jahanifar.

* Corresponding authors.
E-mail addresses: emad.rakha@nottingham.ac.uk (E. Rakha), n.m.rajpoot@warwick.ac.uk (N. Rajpoot).

https://doi.org/10.1016/j.modpat.2023.100416

Introduction

Tumor proliferation has proven to be one of the most powerful prognostic factors, and it is essential for determining a patient's prognostic risk.[1-3] In breast cancer (BC), proliferation is assessed by counting mitotic figures in hematoxylin and eosin (H&E)-stained sections, which is a critical component of the Nottingham grading system and a well-recognized histomorphologic predictor of outcome.[4-6]

The introduction of digital pathology allowed the use of automated tools for quantifying mitotic figures in scanned slides, which can provide an aid to pathologists in routine practice.[7,8] In recent years, the performance of artificial intelligence (AI) algorithms has shown marked improvement, which is comparable to that of expert pathologists, adding more consistency in detecting mitotic figures.[9,10]

However, to validate the use of such algorithms in routine practice, not only the sensitivity and specificity of detecting mitotic figures are essential but also the method of scoring has to be established and validated to best represent the proliferative activity of the tumor. The identification of the most prognostically relevant mitosis scoring technique is an area that requires further study and investigation.

Different techniques have been proposed to visually estimate mitotic counts, and these include mitotic index (MI), mitotic activity index (MAI), and mitotic count per tumor (MCT).[8]However, MI is commonly defined as the ratio of mitotic cells to nonmitotic cells of a tumor and is reported as a percentage or the number of mitoses per 1000 neoplastic cells.[11] Because it is not region-specific, it overcomes challenges associated with differences in tumoral cellularity, intratumoral stroma, and cell size; however, its usefulness in routine practice is less well studied and is restricted by the fact that it is exceedingly laborious and time-consuming.[8] MAI, on the other hand, is described as the number of mitotic figures in a specified area of a tumor, chosen as having the highest number of mitotic figures (hotspot),[12] and it is provided as an index (mitotic count/area).[3,11,13] In BC, using conventional light microscopes, the optimal area size is that of 10 high-power fields (HPF), but it varies based on the diameter of the microscope field.[12] Most modern microscopes have a field diameter of approximately 0.055 mm, with 10 HPF covering an area of 2.37 mm^2.[8] In a previous study to define the area of mitoses counting, 3 mm^2 was reported as the optimal area associated with high reproducibility and outcome correlation.[14] This method is time efficient and often reflects the most replicative capacity of the tumor,[12] despite the interobserver variation in the selection of these areas.[15] Finally, MCT is often expressed as the number of mitoses per area occupied by invasive tumor cells, rather than the number of mitoses per specific area or HPF, which could alleviate the subjectivity of area selection.[16,17] Nevertheless, none of these methods has been proven to outperform the others in a large-scale study.

This study aimed to determine the optimal mitosis scoring method in BC and evaluate the performance of the automated mitotic score for survival prediction compared with visual scores. We provide an insight into the feasibility of using automated mitosis counting in clinical practice and its potential advantages over visual scoring.

Material and Methods

Study Cohorts

This study includes 2 separate cohorts—one for discovery and internal validation and the other one for external multicentric validation.

Nottingham Cohort

This is a large cohort of primary invasive estrogen receptor-positive (ER+)/human epidermal growth factor receptor 2-negative (HER2−) BC ($n = 2574$) cases that were diagnosed and treated at the Nottingham City Hospital, Nottingham, United Kingdom. Ninety-three percent of the patients received endocrine therapy. Classical treatment of cyclophosphamide, methotrexate, and 5-fluorouracil was used as a therapy for patients clinically fit to receive chemotherapy. None of the patients in the current study cohort received neoadjuvant therapy.

Clinical information and tumor characteristics, including patient's age at diagnosis, histologic tumor type, grade, tumor size, lymph node status, Nottingham prognostic index, and lymphovascular invasion were available.[18] Data for ER, progesterone receptor, HER2, and Ki67 were available as previously published.[19-22] Hormonal and HER2 statuses were assessed according to the American Society of Clinical Oncology and College of American Pathologists guidelines.[23] The Ki-67 scoring was evaluated visually using the global (average) method, following the recommendations of the International Ki67 in Breast Cancer Working Group. A minimum of 3 high-power (×40 objective) fields that represented the staining spectrum observed in the entire section were selected, with a particular focus on scoring the invasive tumor edge. Data from hotspots were incorporated into the overall score, and only nuclear staining was considered positive, with staining intensity not taken into account. Ideally, at least 1000 malignant invasive cells were considered for scoring[24] and were defined as high when ≥14% of tumor cells showed nuclear positivity.[25]

The outcome data collected for the study included BC-specific survival (BCSS), distant metastasis-free survival (DMFS), and recurrence-free survival (RFS), all measured in months. BCSS was defined as the time from the date of primary surgical treatment until the time of death due to BC, DMFS was defined as the time from surgery until the first event of distant metastasis, and RFS was defined as the time from surgical resection until disease recurrence.

Pseudonymized patient tissue samples were provided. One representative tissue block (formalin-fixed and paraffin-embedded), with adequate tumor tissue, was chosen per case. Four-micrometer-thick, full-face tumor sections were cut and stained with H&E. The slides were scanned with a Philips UFS scanner with 0.25 μm/pixels at 40× and Pannoramic 250 Flash III: 3DHistech (0.19 μm/pixel), generating high-quality whole slide images (WSIs).

The Nottingham cases were divided into a discovery set ($n = 1715$) and a validation set ($n = 859$), based on stratified random distribution of events (Supplementary Fig. S1). In the discovery cohort, the median survival duration was 89 months (IQR, 37.3-179), whereas in the validation group, the median survival duration was 71.3 months (IQR, 51.9-124.9). The cutoff values generated in the discovery set were applied to the internal validation and external test sets.

The Cancer Genomic Atlas Breast Cancer Cohort

In this study, the BC cohort of 757 cases from the Cancer Genomic Atlas (https://www.cancer.gov/tcga) was used as an external test set The Cancer Genome Atlas of breast invasive carcinoma (TCGA-BRCA).[26] H&E images were obtained from excision specimens and scanned using various scanners from different institutions across the United States. To ensure the reliability of our analysis, we implemented a quality control measure and excluded images with very low quality, we carefully selected 757 cases, specifically focusing on those with the best available image

quality. WSIs were downloaded from the genomic data commons (GDC) data portal https://portal.gdc.cancer.gov/.[27] Clinical data were available from the https://portal.gdc.cancer.gov/, https://www.cbioportal.org/, https://ucsc-xena.gitbook.io/project/.[27-30] Comprehensive clinical data including age, tumor size, grade and its components, histologic tumor subtypes, pathological stage, ER/progesterone receptor status, lymphovascular invasion, and Ki67 score were extracted from the TCGA cohort. Overall survival and RFS data were also included in the analysis where median survival time was 31 months (IQR, 17-60 months).

Algorithm Development

Annotations

In order to create machine learning (ML) models for mitosis detection, cell-level annotations were made. A group of 6 certified pathologists from Nottingham were provided with an online annotation software, called WASABI.[31] This application offers specialized modes that are designed to facilitate the annotation of WSIs. Pathologists were responsible for performing the primary annotations of various phases and morphologies of mitotic figures (prophase, metaphase, anaphase, and telophase, as well as atypical mitotic figures), in addition to identifying mimickers such as lymphocytes, stromal cells, and artifacts.

Two pathologists were assigned to independently annotate mitotic figures for each WSI in a blinded manner, (A.I. and A.K.) as previously described.[31-33] Any ambiguous cases or disagreements were re-evaluated by another pathologist to establish a consensus label. Through this approach (as depicted in Fig. 1A), a total of 7916 mitotic figures were manually annotated.

Mitosis Detection Algorithm

The method used for mitosis detection follows a well-established 2-stage framework developed by Jahanifar et al.[34] The framework consists of mitosis candidate segmentation and candidate refinement stages (Fig. 1B). The first stage uses a fast and accurate convolutional neural network to segment mitotic candidates. To train the segmentation network, a mitosis mask was generated based on pathologist point annotations and an interactive annotation tool called NuClick.[35] In the second stage, the candidate refinement is performed using a deeper classifier network. Both stages are domain-invariant, making the framework robust against domain shift.

The algorithm used in this study has been validated extensively for the task of mitosis detection from various cancer images (ranked first in Mitosis Domain Generalization Challenges 2021-2022[9,10]). We have also evaluated the performance of the mitosis detection algorithm on a data set of 9200 tile images (512 × 512 pixels in size) as an initial part of the study. This data set was curated based on visual mitosis and mimicker annotations. Human correction has also been implemented, where pathologists with experience in the field (A.I., M.T., A.K., and A.L.) reviewed, corrected, and confirmed the mitotic figures identified by the algorithm in a subset of cases. In cross-validation experiments, the utilized algorithm achieved an F1-score of 0.93, sensitivity of 0.89, and precision of 0.97, demonstrating high performance in the mitosis detection task.

Artificial Intelligence-Assisted Identification of Mitotic Hotspot Regions

A computational framework was developed to objectively identify regions of mitotic hotspots using a greedy search algorithm (Fig. 1C). First, the algorithm identifies the tissue region within each WSI by employing a tissue segmentation convolutional neural network from TIAToolbox.[36] Next, it extracts 512 × 512 tiles from the tissue region, each with a 50-pixel overlap, at a resolution of 0.25 microns-per-pixel (equivalent to a ×40 objective magnification). Then, the method described in the previous section is applied to detect mitoses in the extracted patches. Once the detection of mitosis is complete, the algorithm performs an overlapping window search within the WSI to identify the mitotic hotspot region, which is defined as the window containing the highest number of mitoses. The heatmap overlay shown in Figure 1C indicates windows with high- and low-mitotic counts with red and blue colors, respectively. Finally, the mitotic score for the hotspot is calculated according to the method outlined in the next section.

Mitosis Scoring Approaches

In order to establish the best mitosis scoring approach, the mitosis detection algorithm was run on the discovery cohort (1725 WSIs), and the number of detected mitotic figures in each digital slide was recorded. MCT was determined by dividing the number of mitotic figures by the whole tumor size in mm^2. Additionally, MI was computed by first utilizing a deep learning-based nuclei instance identification model called HoVer-Net[37] to quantify the number of malignant tumor cells present in the entire slide, followed by calculating the average number of mitotic figures per 1000 malignant cells. Finally, MAI was calculated by counting the number of mitotic figures within a 3 mm^2 hotspot region of the slide. The 3 mm^2 area was carefully chosen to capture the invasive carcinoma cells avoiding the inclusion of noninvasive stromal tissue or ductal carcinoma in situ (DCIS). However, if the hotspot was near the leading edge, multiple separate annotated areas collectively measuring 3 mm^2 were used.[14]

The study deliberately used the same mitosis detection algorithm for all 3 scoring systems to ensure an unbiased comparison; therefore, we did not detect systematic differences when comparing different mitosis scoring approaches. The mitosis scoring techniques were evaluated and compared based on their correlation with clinicopathologic parameters, the established gold standard visual scoring method used in clinical practice, Ki67 score, patient outcome, and chemotherapy prediction.

Measuring the Correlation Between Visual and Automated Mitosis Detection

To confirm the reliability and reproducibility of automated mitosis detection, a well-trained pathologist visually counted mitotic figures within 3 mm^2 in 400 cases from the Nottingham validation set and 757 from the external validation set as continuous counts following the proposed scoring method.[38] Scoring was carried out blindly. The visual counts were correlated with their parallel automatically generated mitotic counts.

Statistical Analysis

Statistical analyses were performed using SPSS v26 for Microsoft Windows. The degree of interobserver agreement was assessed by use of the intraclass correlation coefficient for continuous data. Cohen's statistics were used to assess the concordance between 2 observers for categorical variables,

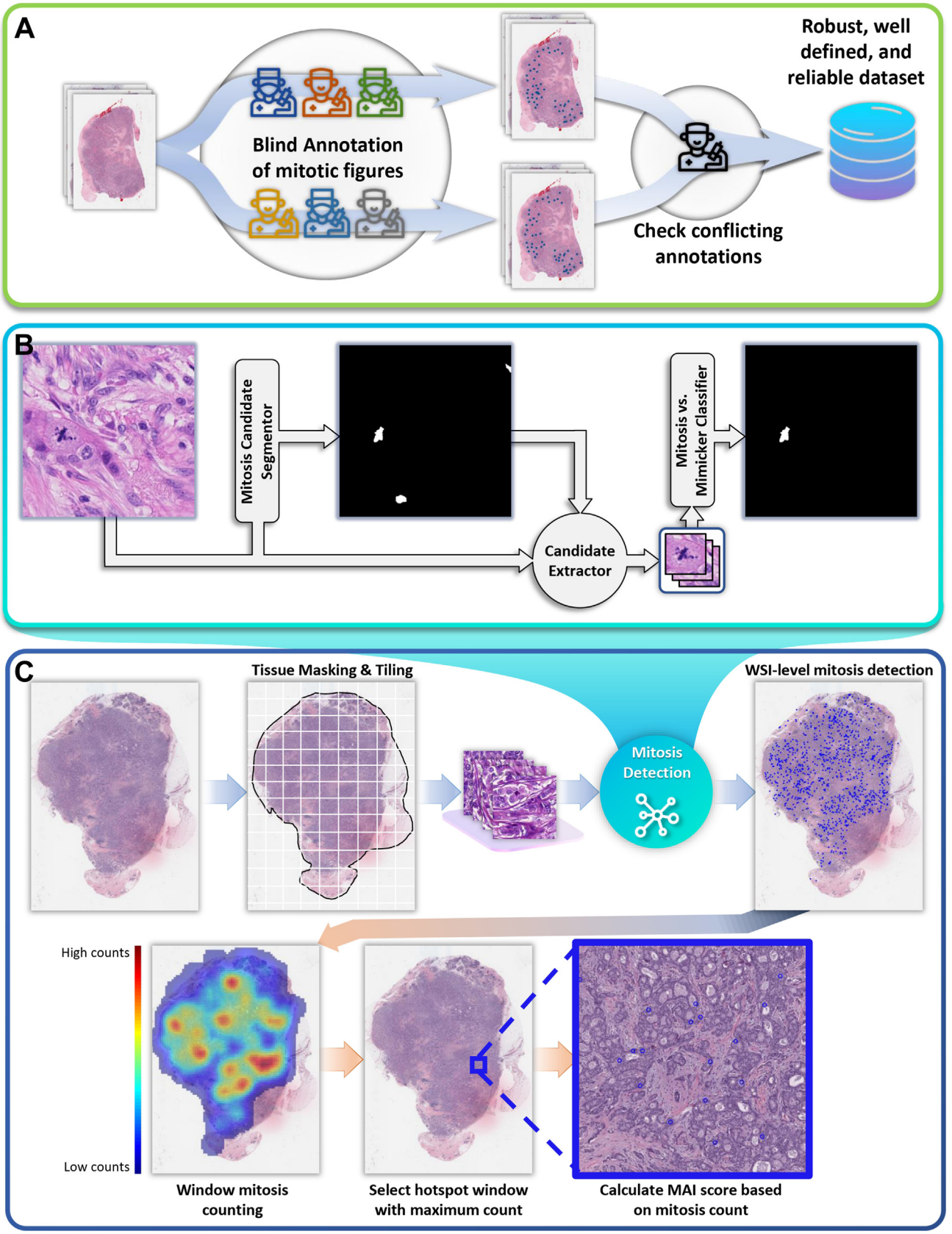

Figure 1.
(A) The process of mitosis annotation in whole slide images. (B) Mitosis candidate segmentation and candidate refinement stages. (C) A computational framework showing the steps for identifying regions of mitotic hotspots, with the heatmap overlay.

whereas Fleiss Kappa was used for more than 2 variables/scores. The correlations between categorical variables were analyzed using the χ^2 test. Pearson's correlation coefficient was used to measure the strength of a linear association between 2 continuous variables. Association with mitosis count and BCSS was performed after classification of expression into high, intermediate, and low groups based on the cutoff point obtained from the x-tile.[39] Survival rates were determined using the Kaplan–Meier method and compared by the log-rank test. Multivariate analysis using the Cox regression model determined the influence of each mitosis scoring technique on survival when compared with one another. All tests were 2-tailed, and a P value of <.05 was considered statistically significant. Finally, the automated MAI scores were incorporated with the other 2 components of the Nottingham grading system (tubule formation and pleomorphism) to develop a grade based on the automated MAI score.

Results

Evaluating Mitosis Scoring Techniques

Automatically derived mitotic counts using the 3 methods (MCT, MI, and MAI) were different, and all showed unimodal distribution. These distributions showed significant variations in the mitotic count of individual cases. The median mitoses count for each method is presented in Supplementary Table S1. These counts were converted into 3 scores with different cutoff values based on BCSS, using x-tiles as follows:

$$MCT - Score = \begin{cases} 1(low), & MCT \leq 110 \\ 2(Intermediate), & 110 < MCT \leq 284 \\ 3(high), & MCT > 284 \end{cases} \quad (1)$$

$$MI - Score = \begin{cases} 1(Low), & MI \leq 2.9 \\ 2(Intermediate), & 2.9 < MI \leq 5.5 \\ 3(High), & MI > 5.5 \end{cases} \quad (2)$$

$$MAI - Score = \begin{cases} 1(Low), & MAI \leq 23 \\ 2(Intermediate), & 23 < MAI \leq 50 \\ 3(High), & MAI > 50 \end{cases} \quad (3)$$

Correlation With Clinicopathologic Parameters

As reported in Supplementary Tables S2-S4, high values of all automatically derived mitotic scores (MAI, MCT, and MI) were significantly associated with characteristics of aggressive tumor behavior including less tubule formation, high nuclear pleomorphism, large tumor size, and high Nottingham prognostic index scores ($P < .001$).

The same results were observed in the validation cohort when the same cutoff values (derived from the discovery cohort) were applied.

Correlation With Ki67 Score

A significant positive linear correlation was observed between the Ki-67 score and both MAI (r = 0.69; $P < .001$) and MCT (r = 0.55; $P < .001$), but no such correlation was found with MI. Similar results were observed in the internal validation cohort and external validation set (Fig. 2).

Correlation With the Well-Established Visual Scoring Method Used in Clinical Practice (Gold Standard)

As shown in Figure 3A and B, statistically significant correlations were observed between pathologist mitotic counts (visual MAI used in clinical practice) and automated MAI for both the Nottingham cohort and the TCGA-BRCA cohort (r = 0.8; $P < .001$), respectively.

Furthermore, automated MCT showed a significant correlation with pathologist mitoses counts (visual MAI, derived from visually identified hotspots in clinical practice) with a Pearson's correlation coefficient of 0.7 ($P < .001$). This implies that the automated mitosis detection algorithm performed reliably on the WSI level as the number of detected mitoses correlates with the visual mitosis count in the mitotic hotspot (which is an indicator of mitotic activity in the whole tumor) (Fig. 3C). On the other hand, there was no significant correlation between pathologist mitoses counts and automated MI (as seen in Fig. 3D)

Prediction of Patient Outcome

Univariate survival analysis revealed that high MCT, MAI, and MI scores were significantly associated with worse BCSS and shorter DMFS (Supplementary Table S5).

However, high MAI and MCT scores were predictive of BC recurrence, whereas MI was not (P =.07). Detailed results and Kaplan-Meier survival plots for mitosis scoring methods across different survival analyses can be found in Figure 4.

Furthermore, a multivariate Cox regression model adjusted for other prognostic covariates (nuclear pleomorphism, tubule formation, nodal stage, and Ki67 score) revealed that MAI, MCT, and MI scores were independent predictors of survival as reported in Table 1, highlighting the significance of mitosis score in predicting the tumor behavior and patient survival.

A multivariate analysis that included all 3 mitosis-related scores as continuous variables was also conducted. The results are reported in Table 2, which showed that MAI was an independent predictor of survival in terms of BCSS, DMFS, and RFS, whereas the other 2 scores (MCT and MI) were not.

When various AI-based mitosis scoring methods were evaluated for predicting outcomes in the context of adjuvant chemotherapy, all 3 methods were strongly associated with outcomes in chemotherapy-naive patients. In patients who were given adjuvant chemotherapy, only MAI remained associated with outcome (HR, 2.35; 95% CI, 1.88-2.93; $P < .001$), whereas MCT and MI lost their significance (Supplementary Fig. S2).

Additionally, as seen from the survival curve, patients with a MAI score of 2 who received chemotherapy demonstrated improved outcomes compared with those with a score of 1, whereas patients with a score of 3 continued to show the worst prognosis.

The results suggest that MAI would be an effective approach in scoring mitosis during routine diagnosis. Therefore, the following sections will focus on the use of MAI for clinicopathologic parameters correlation and survival prediction.

Visual Versus Automated Mitotic Activity Index for Clinicopathologic Correlation and Survival Prediction

The results from the external test set (Table 3) and the Nottingham cohort (Supplementary Table S6) revealed a significant correlation between aggressive tumor characteristics and high visual and automated MAI values. Regarding association with the outcome, both automated and visual MAI were predictors of survival in the Nottingham and TCGA cohorts, as depicted in the Kaplan-Mayer survival plots in Supplementary Figure S3.

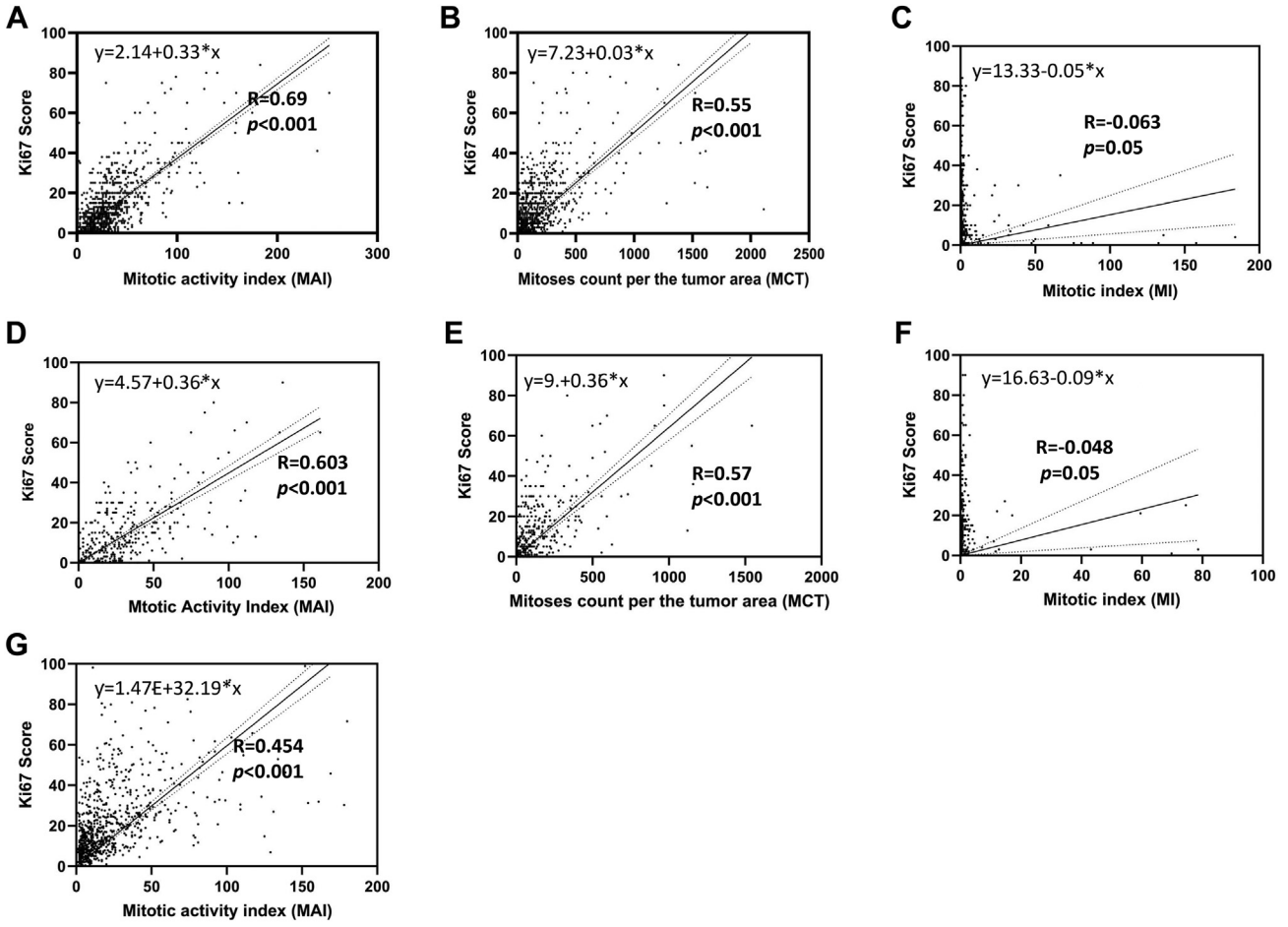

Figure 2.
The correlation between Ki67 score and 3 measures of mitotic activity. (A) The correlation between Ki67 score and mitotic activity index (MAI). (B) The correlation between Ki67 score and mitotic count per the whole tumor (MCT). (C) The correlation between Ki67 score and mitotic index (MI) in the discovery cohort, in addition to (D) the correlation between Ki67 score and MAI. (E) The correlation between Ki67 score and MCT, and (F) the correlation between Ki67 score and MI in the internal validation cohort. (G) Finally, the correlation between Ki67 score and MAI in the external validation set.

Automated Mitotic Activity Index and Nottingham Grading System

The addition of automated MAI to the tubule formation and pleomorphism scores in the *Nottingham grade* was found to have a significant association with BCSS, exhibiting a slightly higher hazard ratio (HR, 3.305; 95% CI, 2.59-4.21; $P < .001$) than the original grade with visual MAI score (HR, 2.8; 95% CI, 2.29-3.64; $P < .001$) as shown in Figure 5. A cross-comparison between new grade and conventional grade was conducted using χ^2 tests, and we found that they were strongly correlated ($\chi^2 = 2990$; $P < .001$). These results highlight the reliability of using AI-assisted mitosis scores in clinical practice.

Discussion

Digital pathology (DP) is an emerging field that involves scanning glass slides used for diagnosis into digital images in clinical settings. Whole slide scanners are used to generate high-resolution images that can be navigated and analyzed using specialized software and automated algorithms. DP has the potential to improve the accuracy and efficiency of diagnostic processes and is being increasingly adopted in medical practice.[7] The introduction of these algorithms has led to numerous attempts by researchers to enhance and integrate this new technology into diagnostic processes. As this field advances, AI is gradually moving from a research tool to a clinical application.[40] The laborious task of visually counting mitotic figures during grading, coupled with the low level of agreement among pathologists has made it a suitable target for computer-assisted detection algorithms.[41] These detection methods are continually improving at a rapid pace. However, the first priority should be the adoption of evidence-based and clinically approved protocols. In BC histopathology, mitosis detection on H&E slides has been extensively researched due to the prognostic value of mitotic density.[22] Because it is an essential part of the grading system, accurate detection of mitotic figures is crucial for patient care. Several studies have shown that AI can count mitoses with great precision,[42] which makes it a promising solution to overcome the challenges of the labor-intensive and subjective nature of visual mitosis counting. Despite several ways to count mitosis have been offered in clinical settings, their challenging applicability has limited their use.[8] The adoption of AI-assisted mitosis counting can improve diagnostic accuracy and reproducibility and facilitate the incorporation of mitotic density into the grading system.

To the best of our knowledge, this is the first large-scale study that has evaluated different mitosis scoring methods with the help

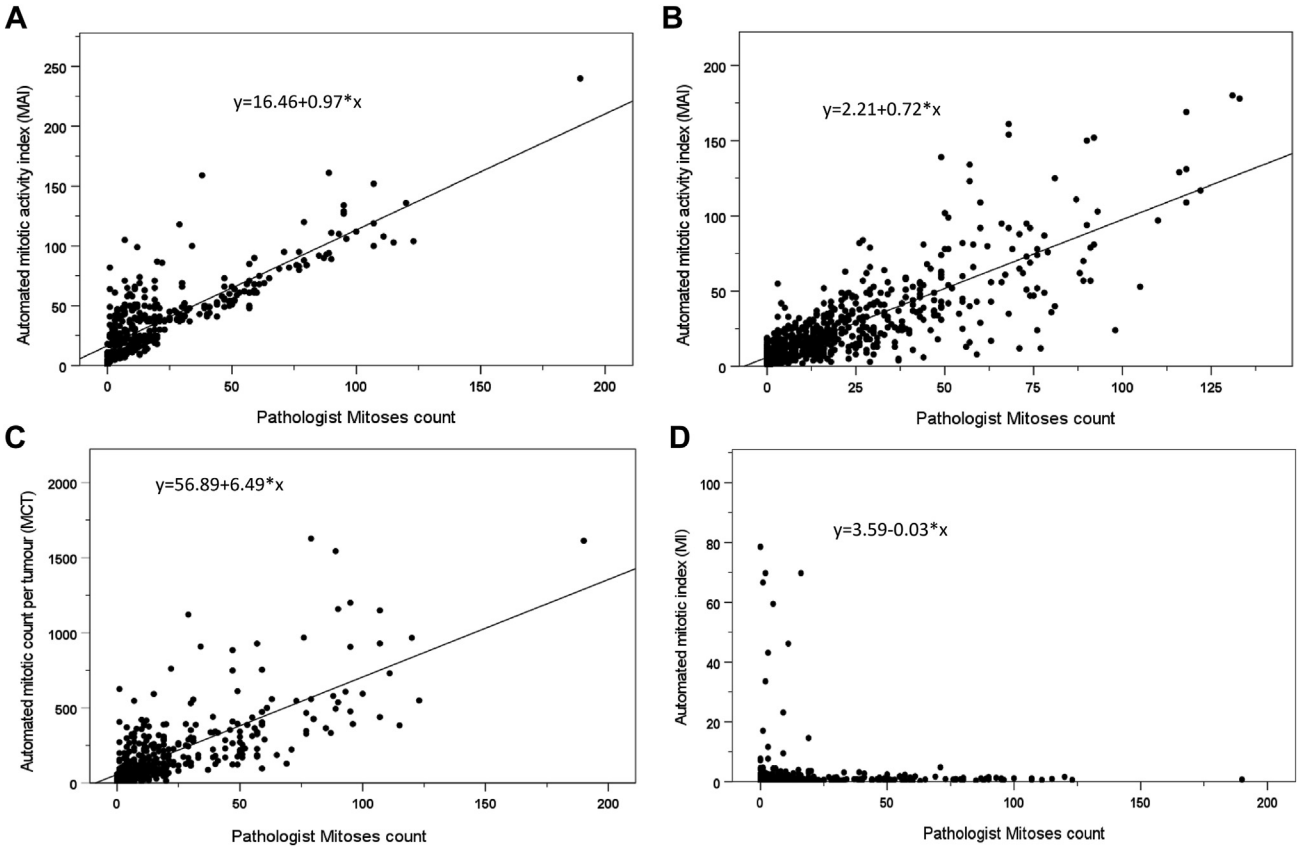

Figure 3.
The correlation between the visual scoring method used in clinical practice with (A) automated MAI in Nottingham cohort, (B) automated MAI in TCGA cohort, (C) MCT in Nottingham cohort, and (D) MI in the Nottingham cohort. TCGA, The Cancer Genome Atlas.

of an AI mitosis detection algorithm in a clinical setting including 2 separate large BC cohorts. The current study, conducted on a large cohort of patients, demonstrates that the automated MAI has the same and, in some cases, greater ability to measure BC proliferative capacity compared with conventional mitotic count (MCT) and MI. This finding is consistent with the results of several other studies, including those conducted by Diest et al,[13] Bostock,[43] Wilcock and Peiffer,[44] Baak et al,[6] and Jannink et al,[45] which have established mitotic count as a reliable predictor of tumor behavior.

The visual counting of mitotic figures throughout the whole tumor has been challenging to implement in practice. As an alternative, the MAI has been proposed as a more feasible parameter.[45] MAI represents the total number of mitotic figures counted within a specified area, enabling rapid and accurate assessment of tumor mitotic activity, without considering cellularity. Moreover, in univariate and multivariate analyses of human breast tumors, MAI was found to be significantly associated with prognosis.[45]

Previous studies concluded that MAI is the preferred index due to its ease of application, time efficiency, and its prognostic value compared with other indices.

The challenges associated with the manual counting of mitotic figures in histopathology have recently come to light as AI tools are being used to count mitoses in digital WSI.[16,19,46]

Our results were similar to those of Jannink et al,[45] where both mitotic count and mitoses per area were significantly associated in linear regression with the other proliferation parameters.

The only parameter that takes cellularity into account is MI, which expresses the number of mitoses as a percentage or referenced to a specific number (1000) of cells.[47-51] However, it has been widely criticized for supposed irreproducibility.[52] Another drawback of MI is the time-consuming task of counting cells in each field.[53] Although there are quicker alternatives such as specific formulas[54] or image analysis techniques,[55] these still have limitations in their application. With the aid of AI, counting mitotic figures can be more easily and accurately performed on a large number of cases, as demonstrated in our study. However, tumors with similar values of cellularity do not necessarily need correction because equal areas may contain similar numbers of cells, and mitotic activity is only due to the proliferative state, not cell content. Other studies suggest that correcting the mitotic count is otherwise unnecessary.[45] On the contrary, a correction might be helpful for those tumors characterized by a high degree of variability in cellularity.

Our study found that MCT, MI, and MAI scores were all correlated with survival. However, the multivariate Cox regression analysis revealed that MAI was an independent predictor of survival. Moreover, only MAI was capable of predicting the outcome in patients receiving chemotherapy in ER+/HER2− patients. Furthermore, the visual evaluation of pathologists was highly correlated with the mitotic figure counts obtained by the automated algorithm.

The 3 parameters expressing mitotic activity were compared with Ki67, which is a widely accepted proliferation marker, to assess their performance. The Ki67 score was strongly correlated with MAI and MCT, but not with MI. We found that both automated and visual MAI values showed a significant correlation with

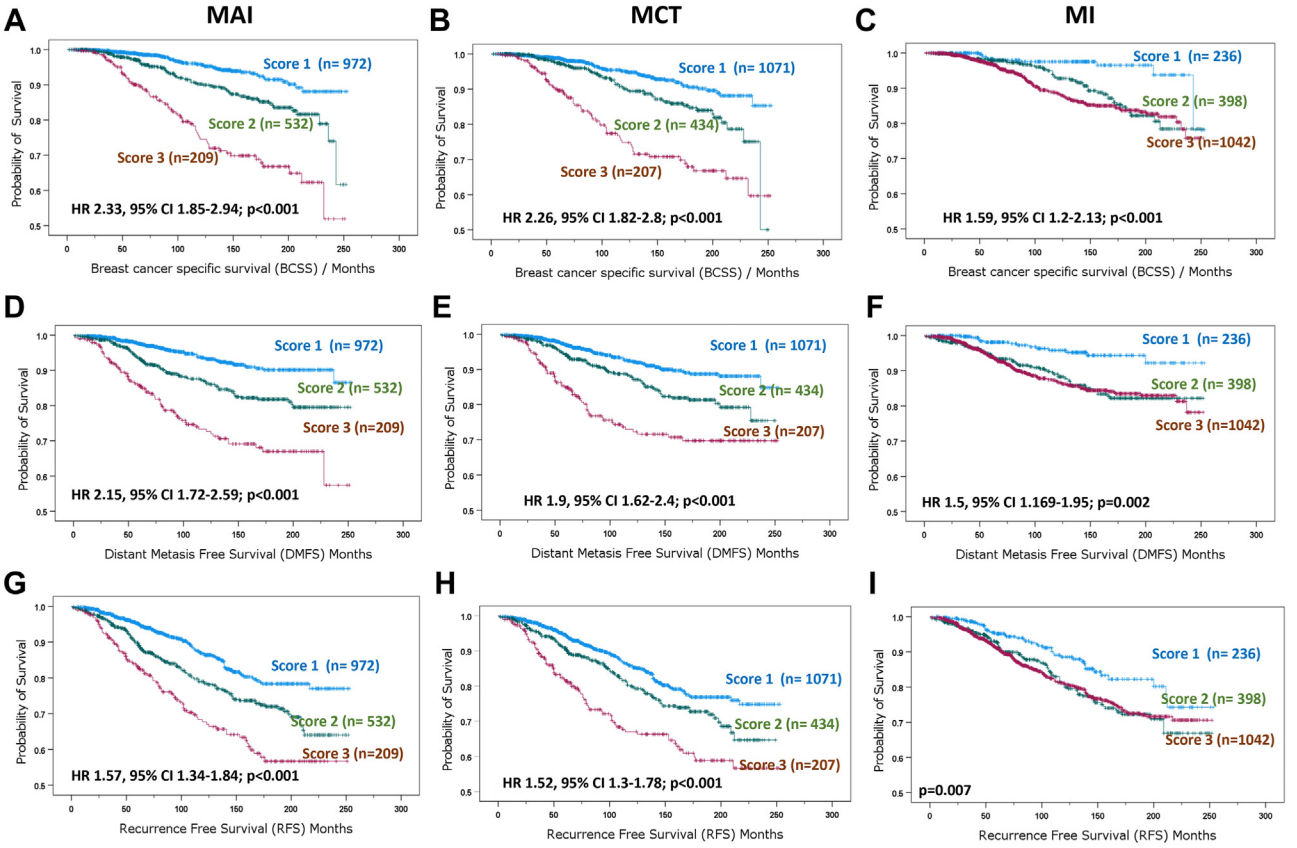

Figure 4.
Kaplan–Meier survival plots for mitosis scoring methods across different survival analysis tasks, such as association of breast cancer-specific survival (BCSS) with (A) MAI, (B) MCT, and (C) MI. The association between these scoring methods and distant metastasis-free survival (DMFS) is presented for (D) MAI, (E) MCT, and (F) MI, respectively. (G-I) Association between the same mitosis scoring methods and recurrence-free survival (RFS).

Table 1
Multivariate Cox regression analysis for predictors of BCSS after adding (A) MCT, (B) MAI and (C) MI

Parameters	Nottingham cohort			
	Hazard ratio (HR)	95% CI for HR		*P* value
		Lower	Upper	
MCT				
Tumor size	1.358	0.938	1.965	.105
Tubular formation	1.836	1.276	2.640	.001[a]
Nuclear pleomorphism	1.713	1.120	2.620	.013[a]
Nodal stage	1.757	1.225	2.520	.002[a]
Ki67 score	0.989	0.663	1.474	.956
MCT	1.627	1.262	2.099	<.001[a]
MAI				
Tumor size	1.304	.897	1.895	.165
Tubular formation	1.822	1.267	2.620	.001[a]
Nuclear pleomorphism	1.780	1.167	2.716	.007[a]
Nodal stage	1.800	1.253	2.586	.001[a]
Ki67 score	0.939	0.615	1.435	.773
MAI	1.631	1.217	2.186	.001[a]
MI				
Tumor size	1.350	.924	1.974	.121
Tubular formation	1.972	1.350	2.879	<.001[a]
Nuclear pleomorphism	1.973	1.294	3.008	.002[a]
Nodal stage	1.673	1.153	2.429	.007[a]
Ki67 score	1.318	0.893	1.946	.165
MI	1.416	1.051	1.909	.022

[a] $P < .05$

BCSS, breast cancer specific survival; MAI, mitotic activity index; MCT, mitosis count per the tumor area; MI, mitotic index.

aggressive breast tumor characteristics and were associated with survival. Additionally, adding automated MAI to the Nottingham grading system improved the association with BCSS and highlighted the reliability of AI-assisted mitosis scores in clinical practice. Additionally, a recent study found strong correlations between different mitotic scoring modalities, including light microscopy, WSI, and AI in both biopsy and resection samples with a

Table 2
Multivariate Cox regression model including the 3 scoring methods (MAI, MCT, and MI) against BCSS, DMFS, and RFS in the discovery cohort

	Hazard ratio (HR)	95% CI for HR		*P* value
		Lower	Upper	
BCSS				
MAI	1.010	1.003	1.017	.007[a]
MCT	1.001	0.988	1.013	.934
MI	1.000	1.000	1.001	.315
DMFS				
MAI	1.011	1.004	1.018	.001[a]
MCT	1.002	0.991	1.013	.774
MI	1.000	0.999	1.001	.558
RFS				
MAI	1.008	1.003	1.014	.005[a]
MCT	1.004	0.996	1.012	.302
MI	1.000	0.999	1.001	.974

[a] $P < .05$

BCSS, breast cancer specific survival; DMFS, distant metastasis-free survival; MAI, mitotic activity index; MCT, mitosis count per tumor area; MI, mitotic index; RFS, recurrence-free survival.

Table 3
Association between automated and visual MAI with the clinicopathologic parameters in the external validation set (TCGA), ($n = 757$)

	Automated MAI				Visual MAI			
	Low score No (%)	Intermediate score No (%)	High score No (%)	χ^2 *P* value	Low score No (%)	Intermediate score No (%)	High score No (%)	χ^2 *P* value
Patient age (y)								
<50	132 (26.0)	42 (25.8)	33 (37.9)	5.549	87 (24.9)	38 (23.3)	82 (33.5)	6.985
≥50	375 (74.0)	121 (74.2)	54 (62.1)	.062	262 (75.1)	125 (76.7)	163 (66.5)	.03[a]
Tumor size								
<2	113 (31.3)	21 (16.5)	10 (14.3)	16.248	67 (27.5)	36 (29.0)	41 (21.6)	2.795
≥2	248 (68.7)	106 (83.5)	60 (85.7)	<.001[a]	177 (72.5)	88 (71.0)	149 (78.4)	.247
Tumor grade								
1	70 (31.5)	2 (2.8)	0 (0.0)	174.159	65 (41.4)	5 (7.5)	2 (1.6)	198.338
2	117 (52.7)	15 (21.1)	0 (0.0)	<.001[a]	85 (54.1)	30 (44.8)	17 (13.8)	<.001[a]
3	35 (15.8)	54 (76.1)	54 (100.0)		7 (4.5)	32 (47.8)	104 (84.6)	
Tubular formation								
1	12 (3.8)	0 (0.0)	0 (0.0)	16.159	12 (5.6)	0 (0.0)	0 (0.0)	22.569
2	61 (19.6)	15 (13.8)	3 (5.0)	.003[a]	41 (19.2)	21 (20.0)	17 (10.5)	<.001[a]
3	239 (76.6)	94 (86.2)	57 (95.0)		161 (75.2)	84 (80.0)	145 (89.5)	
Pleomorphism								
1	26 (8.7)	0 (0.0)	0 (0.0)	127.653	24 (12.2)	2 (1.9)	0 (0.0)	141.584
2	173 (58.1)	16 (15.1)	4 (7.0)	<.001[a]	124 (63.3)	46 (44.7)	23 (14.2)	<.001[a]
3	99 (33.2)	90 (84.9)	53 (93.0)		48 (24.5)	55 (53.4)	139 (85.8)	
Histologic subtypes								
Non-specific type (NST)	315 (62.1)	145 (88.3)	77 (87.4)	90.675	199 (57.7)	120 (77)	218 (90)	118.240
Invasive lobular	139 (27.4)	8 (4.9)	5 (5.7)	<.001[a]	116 (33.6)	24 (15.3)	12 (5)	<.001[a]
Mixed NST and special type	13 (2.6)	1 (0.6)	0 (0.0)		19 (5.5)	10 (6.4)	11 (4.6)	
Other special types[b]	32 (6.4)	6 (6.2)	5 (6.9)		11 (3.2)	2 (1.3)	1 (0.4)	
Lymph node involvement					74 (21.2)	30 (18.4)	42 (17.1)	
Negative	114 (22.5)	22 (13.5)	10 (11.5)	12.160	194 (55.6)	97 (59.5)	146 (59.6)	1.902
Positive	277 (54.6)	100 (61.3)	60 (69.0)	.016[a]	81 (23.2)	36 (22.1)	57 (23.3)	.754
Lymphovascular invasion								
Negative	351 (69.2)	86 (52.8)	58 (66.7)	14.855	249 (71.3)	99 (60.7)	147 (60.0)	10.177
Positive	156 (30.8)	77 (47.2)	29 (33.3)	.001[a]	100 (28.7)	64 (39.3)	98 (40.0)	.006[a]
Progesterone receptor								
Negative	113 (23.0)	71 (45.5)	60 (74.1)	94.503	69 (20.3)	45 (29.4)	130 (55.1)	77.154
Positive	379 (77.0)	85 (54.5)	21 (25.9)	<.001[a]	271 (79.7)	108 (70.6)	106 (44.9)	<.001[a]
Ki67 index								
Low	384 (75.7)	99 (60.7)	37 (42.5)	44.198	281 (80.5)	107 (65.6)	132 (53.9)	48.393
High	123 (24.3)	64 (39.3)	50 (57.5)	<.001[a]	68 (19.5)	56 (34.4)	113 (46.1)	<.001[a]

[a] $P < .05$
[b] Other special types: mucinous, tubylar, and papillary.
MAI, mitotic activity index; TCGA, The Cancer Genome Atlas.

high level of agreement. These findings highlight the reliability and consistency of these modalities for mitotic counting and BC grading in clinical practice.[56]

The use of AI technology for evaluating BC poses the challenge of standardizing the method for mitosis scoring, which requires evidence-based studies to determine the best strategy. As AI-based algorithms for counting mitosis in WSI continue to evolve, they have the potential to revolutionize the assessment of mitotic figures and grading in BC and other diagnostic pathology fields. To ensure the effectiveness and reliability of these algorithms, developers must be familiar with established scoring methods used in BC and adjust their techniques accordingly to provide the same prognostic value when incorporated into the final histologic grade.

The decision to train AI to produce results similar to human visual assessment could be perceived as a potential limitation of the approach taken in this study and that the algorithm never will be better than human visual assessment. However, the current study evaluated AI algorithms for mitosis counting not only to achieve automation and consistency but also the AI algorithm does not replicate the pathologist error. The algorithm has been trained on a data set of mitosis annotations that are obtained from the consensus of multiple pathologists and has demonstrated strong generalization to data from different sources. This has been investigated in Aubreville et al,[9] where the proposed mitosis detection algorithm performed better than 5 individual pathologists in the detection task. The similarity of AI and visual assessment of mitoses counts is only an indicator of reliability of using AI-assisted MAI scores in clinical practice to the same level of pathologist-driven scores.

In the current study, we evaluated the optimal method of mitosis detection in BC using AI as one of the well-known prognostic markers and is a component of BC grade. DP is increasingly used and AI algorithms for assessing several morphologic features including mitosis will become commonplace soon. Our proposed mitosis scoring pipeline can be encapsulated into a single software package, and we have implemented a toolbox that accepts the input from the WSI and runs the whole pipeline on it to detect mitotic hotspots and estimate MAI. At this stage, MAI can be combined with visual assessment of tubule formation and pleomorphism to form the new grade. However, there is ongoing work on automated assessment of tubule formation and nuclear pleomorphism as well, which can be combined with MAI in our score (digital grade), but this still needs further refining and validation.

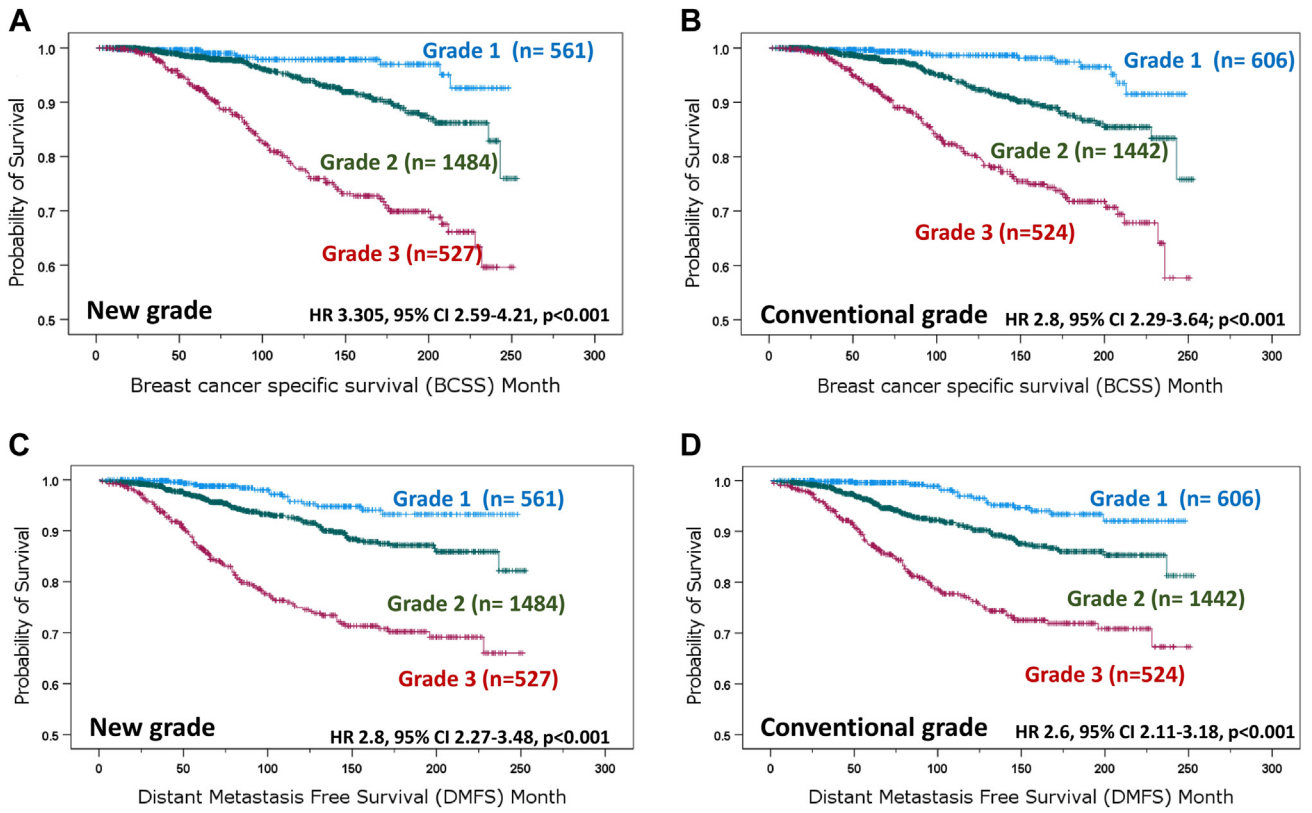

Figure 5.
Kaplan–Meier survival plots show breast cancer-specific survival according to (A) modified grade after replacing mitosis score with automated MAI, (B) conventional Nottingham tumor grade in the whole cohort, in addition to the distant metastasis-free survival according to (C) modified grade after replacing mitosis score with automated MAI, and (D) conventional Nottingham tumor grade in the whole cohort.

Based on our study, it can be concluded that the application of ML algorithms in the quantification of mitotic figures is a promising approach that provides a practical and efficient method for mitosis scoring in BC patients. The use of these algorithms not only overcomes the limitations of visual counting, such as inter-observer variability, but also offers the potential for high-throughput and automated analysis of large data sets.

In addition, we have found that the updated algorithms provide valid measures of scoring in BC patients. The performance of the ML algorithms in the validation cohort demonstrated their ability to accurately detect mitotic figures in a manner that is consistent with visual counting by expert pathologists. This confirms the potential for the use of ML algorithms as a reliable alternative to visual counting for mitotic scoring in BC.

Acknowledgments

The authors are part of the PathLAKE digital pathology consortium. These new centers are supported by the Data to Early Diagnosis and Precision Medicine strand of the government's Industrial Strategy Challenge Fund, managed and delivered by UK Research and Innovation (UKRI). A.I., S.M., N.A., and A.L. are supported and funded by the Egyptian Ministry of Higher Education and Scientific Research.

Author Contributions

A.I. wrote the manuscript draft, data analysis, and interpretation. M.J. devised the mitosis detection algorithm and did the data extraction and helped with manuscript writing. A.I., M.T., A.K., and A.L. helped in annotation. N.R., M.J., A.I., S.M., N.A., M.T., S.G., A.L., W.L., S.G., A.K., M.B., A.B., M.F., S.R., and D.S. critically reviewed the article and agree with manuscript results and conclusions. E.R. conceived and planned the study, contributed to data interpretation, made critical revisions, and approved the final version.

Data Availability

All data used in this study are available and can be accessed upon reasonable request.

Funding

AI is funded by the Egyptian Ministry of Higher Education and Scientific Research.

Declaration of Competing Interest

All the authors declare that they have no conflict of interest.

Ethical Approval and Consent to Participate

Ethical approval was obtained for this study and approved by REC (REF. no. 19/SC/0363) under the title "PathLAKE." All cases included in the study were fully anonymized.

Supplementary Material

The online version contains supplementary material available at https://doi.org/10.1016/j.modpat.2023.100416

References

1. Halabi S, Owzar K. The importance of identifying and validating prognostic factors in oncology. *Semin Oncol*. 2010;37(2):e9–e18. https://doi.org/10.1053/j.seminoncol.2010.04.001
2. van Diest PJ, van der Wall E, Baak JP. Prognostic value of proliferation in invasive breast cancer: a review. *J Clin Pathol*. 2004;57(7):675–681. https://doi.org/10.1136/jcp.2003.010777
3. van Diest PJ, Brugal G, Baak JP. Proliferation markers in tumours: interpretation and clinical value. *J Clin Pathol*. 1998;51(10):716–724. https://doi.org/10.1136/jcp.51.10.716
4. Rakha EA, Reis-Filho JS, Baehner F, et al. Breast cancer prognostic classification in the molecular era: the role of histological grade. *Breast Cancer Res*. 2010;12(4):207. https://doi.org/10.1186/bcr2607
5. Rakha EA, El-Sayed ME, Lee AH, et al. Prognostic significance of Nottingham histologic grade in invasive breast carcinoma. *J Clin Oncol*. 2008;26(19):3153–3158. https://doi.org/10.1200/JCO.2007.15.5986
6. Baak JP. Mitosis counting in tumors. *Hum Pathol*. 1990;21(7):683–685. https://doi.org/10.1016/0046-8177(90)90026-2
7. Jahn SW, Plass M, Moinfar F. Digital pathology: advantages, limitations and emerging perspectives. *J Clin Med*. 2020;9(11). https://doi.org/10.3390/jcm9113697
8. Cree IA, Tan PH, Travis WD, et al. Counting mitoses: SI(ze) matters. *Mod Pathol*. 2021;34(9):1651–1657. https://doi.org/10.1038/s41379-021-00825-7
9. Aubreville M, Stathonikos N, Bertram CA, et al. Mitosis domain generalization in histopathology images—the MIDOG challenge. *Med Image Anal*. 2023;84,102699. https://doi.org/10.1016/j.media.2022.102699
10. Wang X, Zhang J, Yang S, et al. A generalizable and robust deep learning algorithm for mitosis detection in multicenter breast histopathological images. *Med Image Anal*. 2023;84:102703. https://doi.org/10.1016/j.media.2022.102703
11. Sarli G, Benazzi C, Preziosi R, et al. Evaluating mitotic activity in canine and feline solid tumors: standardizing the parameter. *Biotech Histochem*. 1999;74(2):64–76. https://doi.org/10.3109/10520299909066480
12. Tan PH, Ellis I, Allison K, et al. WHO classification of tumours editorial board the 2019 World Health Organization classification of tumours of the breast. *Histopathology*. 2020;77(2):181–185. https://doi.org/10.1111/his.14091
13. van Diest PJ, Baak JP, Matze-Cok P, et al. Reproducibility of mitosis counting in 2,469 breast cancer specimens: results from the Multicenter Morphometric Mammary Carcinoma Project. *Hum Pathol*. 1992;23(6):603–607. https://doi.org/10.1016/0046-8177(92)90313-r
14. Ibrahim A, Lashen AG, Katayama A, et al. Defining the area of mitoses counting in invasive breast cancer using whole slide image. *Mod Pathol*. 2022;35(6):739–748. https://doi.org/10.1038/s41379-021-00981-w
15. Yadav KS, Gonuguntla S, Ealla KK, et al. Assessment of interobserver variability in mitotic figure counting in different histological grades of oral squamous cell carcinoma. *J Contemp Dent Pract*. 2012;13(3):339–344. https://doi.org/10.5005/jp-journals-10024-1148
16. Balkenhol MC, Tellez D, Vreuls W, et al. Deep learning assisted mitotic counting for breast cancer. *Lab Invest*. 2019;99(11):1596–1606. https://doi.org/10.1038/s41374-019-0275-0
17. Tabata K, Uraoka N, Benhamida J, et al. Validation of mitotic cell quantification via microscopy and multiple whole-slide scanners. *Diagn Pathol*. 2019;14(1):65. https://doi.org/10.1186/s13000-019-0839-8
18. Rakha EA, Martin S, Lee AHS, et al. The prognostic significance of lymphovascular invasion in invasive breast carcinoma. *Cancer*. 2012;118(15):3670–3680. https://doi.org/10.1002/cncr.26711
19. Aleskandarany MA, Abduljabbar R, Ashankyty I, et al. Prognostic significance of androgen receptor expression in invasive breast cancer: transcriptomic and protein expression analysis. *Breast Cancer Res Treat*. 2016;159(2):215–227. https://doi.org/10.1007/s10549-016-3934-5
20. Rakha EA, Agarwal D, Green AR, et al. Prognostic stratification of oestrogen receptor-positive HER2-negative lymph node-negative class of breast cancer. *Histopathology*. 2017;70(4):622–631. https://doi.org/10.1111/his.13108
21. Rakha EA, Elsheikh SE, Aleskandarany MA, et al. Triple-negative breast cancer: distinguishing between basal and nonbasal subtypes. *Clin Cancer Res*. 2009;15(7):2302–2310. https://doi.org/10.1158/1078-0432.CCR-08-2132
22. Muftah AA, Aleskandarany MA, Al-Kaabi MM, et al. Ki67 expression in invasive breast cancer: the use of tissue microarrays compared with whole tissue sections. *Breast Cancer Res Treat*. 2017;164(2):341–348. https://doi.org/10.1007/s10549-017-4270-0
23. Wolff AC, Hammond MEH, Hicks DG, et al. Recommendations for human epidermal growth factor receptor 2 testing in breast cancer: American Society of Clinical Oncology/College of American Pathologists Clinical Practice Guideline Update. *J Clin Oncol*. 2013;31(31):3997–4013. https://doi.org/10.1200/JCO.2013.50.9984
24. Urruticoechea A, Smith IE, Dowsett M. Proliferation marker Ki-67 in early breast cancer. *J Clin Oncol*. 2005;23(28):7212–7220. https://doi.org/10.1200/JCO.2005.07.501
25. Goldhirsch A, Wood WC, Coates AS, et al. Strategies for subtypes–dealing with the diversity of breast cancer: highlights of the St. Gallen International Expert Consensus on the Primary Therapy of Early Breast Cancer 2011. *Ann Oncol*. 2011;22(8):1736–1747. https://doi.org/10.1093/annonc/mdr304
26. Wang Z, Jensen MA, Zenklusen JC. A practical guide to the cancer genome atlas (TCGA). *Methods Mol Biol*. 2016;1418:111–141. https://doi.org/10.1007/978-1-4939-3578-9_6
27. Jensen MA, Ferretti V, Grossman RL, Staudt LMe. The NCI Genomic Data Commons as an engine for precision medicine. *Blood*. 2017;130(4):453–459. https://doi.org/10.1182/blood-2017-03-735654
28. Kent WJ, Sugnet CW, Furey TS, et al. The human genome browser at UCSC. *Genome Res*. 2002;12(6):996–1006. https://doi.org/10.1101/gr.229102
29. Karolchik D, Kuhn RM, Baertsch R, et al. The UCSC genome browser database: 2008 update. *Nucleic Acids Res*. 2008;36(Database issue):D773–D779. https://doi.org/10.1093/nar/gkm966
30. Cerami E, Gao J, Dogrusoz U, et al. The cBio cancer genomics portal: an open platform for exploring multidimensional cancer genomics data. *Cancer Discov*. 2012;2(5):401–404. https://doi.org/10.1158/2159-8290.CD-12-0095
31. Wahab N, Miligy IM, Dodd K, et al. Semantic annotation for computational pathology: multidisciplinary experience and best practice recommendations. *J Pathol Clin Res*. 2022;8(2):116–128. https://doi.org/10.1002/cjp2.256
32. Ibrahim A, Lashen A, Toss M, Mihai R, Rakha E. Assessment of mitotic activity in breast cancer: revisited in the digital pathology era. *J Clin Pathol*. 2022;75(6):365–372. https://doi.org/10.1136/jclinpath-2021-207742
33. Lashen A, Ibrahim A, Katayama A, et al. Visual assessment of mitotic figures in breast cancer: a comparative study between light microscopy and whole slide images. *Histopathology*. 2021;79(6):913–925. https://doi.org/10.1111/his.14543
34. Jahanifar M, Shephard A, Zamanitajeddin N, et al. Stain-robust mitotic figure detection for MIDOG 2022 challenge. *arXiv preprint arXiv*. 2022, 2208.12587.
35. Koohbanani NA, Jahanifar M, Tajadin NZ, Rajpoot N. NuClick: a deep learning framework for interactive segmentation of microscopic images. *Med Image Anal*. 2020;65, 101771. https://doi.org/10.1016/j.media.2020.101771
36. Pocock J, Graham S, Vu QD, et al. TIAToolbox as an end-to-end library for advanced tissue image analytics. *Commun Med (Lond)*. 2022;2:120. https://doi.org/10.1038/s43856-022-00186-5
37. Graham S, Vu QD, Raza SEA, et al. Hover-Net: simultaneous segmentation and classification of nuclei in multi-tissue histology images. *Med Image Anal*. 2019;58, 101563. https://doi.org/10.1016/j.media.2019.101563
38. Salgado R, Denkert C, Demaria S, et al. The evaluation of tumor-infiltrating lymphocytes (TILs) in breast cancer: recommendations by an International TILs Working Group 2014. *Ann Oncol*. 2015;26(2):259–271. https://doi.org/10.1093/annonc/mdu450
39. Camp RL, Dolled-Filhart M, Rimm DL. X-tile: a new bio-informatics tool for biomarker assessment and outcome-based cut-point optimization. *Clin Cancer Res*. 2004;10(21):7252–7259. https://doi.org/10.1158/1078-0432.CCR-04-0713
40. Davenport T, Kalakota R. The potential for artificial intelligence in healthcare. *Future Healthc J*. 2019;6(2):94–98. https://doi.org/10.7861/futurehosp.6-2-94
41. Ibrahim A, Gamble P, Jaroensri R, et al. Artificial intelligence in digital breast pathology: techniques and applications. *Breast*. 2020;49:267–273. https://doi.org/10.1016/j.breast.2019.12.007
42. Pantanowitz L, Hartman D, Qi Y, et al. Accuracy and efficiency of an artificial intelligence tool when counting breast mitoses. *Diagn Pathol*. 2020;15(1):80–80. https://doi.org/10.1186/s13000-020-00995-z
43. Bostock DE. Prognosis after surgical excision of canine melanomas. *Vet Pathol*. 1979;16(1):32–40. https://doi.org/10.1177/030098587901600103
44. Wilcock BP, Peiffer Jr RL. Morphology and behavior of primary ocular melanomas in 91 dogs. *Vet Pathol*. 1986;23(4):418–424. https://doi.org/10.1177/030098588602300411
45. Jannink I, Risberg B, Van Diest PJ, Baak JP. Heterogeneity of mitotic activity in breast cancer. *Histopathology*. 1996;29(5):421–428. https://doi.org/10.1046/j.1365-2559.1996.d01-509.x
46. Wang M, Aung PP, Prieto VG. Standardized method for defining a 1-mm2 region of interest for calculation of mitotic rate on melanoma whole slide images. *Arch Pathol Lab Med*. 2021;145(10):1255–1263. https://doi.org/10.5858/arpa.2020-0137-OA
47. Quinn CM, Wright NA. Mitosis counting. In: Hall PA, Levison DA, Wright NA, eds. *Assessment of Cell Proliferation in Clinical Practice*. Springer Japan; 1992:83–94.
48. Woosley JT. Measuring cell proliferation. *Arch Pathol Lab Med*. 1991;115(6):555–557.
49. Hall PA, Levison DA. Review: assessment of cell proliferation in histological material. *J Clin Pathol*. 1990;43(3):184–192. https://doi.org/10.1136/jcp.43.3.184
50. Amin MB, Ma CK, Linden MD, Kubus JJ, Zarbo RJ. Prognostic value of proliferating cell nuclear antigen index in gastric stromal tumors. Correlation with mitotic count and clinical outcome. *Am J Clin Pathol*. 1993;100(4):428–432. https://doi.org/10.1093/ajcp/100.4.428

51. Graem N, Helweg-Larsen K. Mitotic activity and delay in fixation of tumour tissue. The influence of delay in fixation on mitotic activity of a human osteogenic sarcoma grown in athymic nude mice. *Acta Pathol Microbiol Scand A 87a:375-8*. 1979;87A(5):375–378.
52. O'Leary TJ, Steffes MW. Can you count on the mitotic index? *Hum Pathol*. 1996;27(2):147–151. https://doi.org/10.1016/s0046-8177(96)90367-6
53. Saldanha G, Ali R, Bakshi A, et al. Global and mitosis-specific interobserver variation in mitotic count scoring and implications for malignant melanoma staging. *Histopathology*. 2020;76(6):803–813. https://doi.org/10.1111/his.14052
54. Simpson JF, Dutt PL, Page DL. Expression of mitoses per thousand cells and cell density in breast carcinomas: a proposal. *Hum Pathol*. 1992;23(6):608–611. https://doi.org/10.1016/0046-8177(92)90314-s
55. Chieco P, Pagnoni M, Romagnoli E, Melchiorri C. A rapid and simple staining method, using toluidine blue, for analysing mitotic figures in tissue sections. *Histochem J*. 1993;25(8):569–577. https://doi.org/10.1007/BF02388065
56. van Bergeijk SA, Stathonikos N, Ter Hoeve ND, et al. Deep learning supported mitoses counting on whole slide images: a pilot study for validating breast cancer grading in the clinical workflow. *J Pathol Inform*. 2023;14, 100316. https://doi.org/10.1016/j.jpi.2023.100316